Phase transitions of the water–xanthan system

Hirohisa Yoshida
Department of Industrial Chemistry, Tokyo Metropolitan University, 2-1-1 Fukazawa, Setagaya-ku, Tokyo 158, Japan

Tatsuko Hatakeyama
Research Institute for Polymers and Textiles, 1-1-4 Higashi, Tsukuba, Ibaraki 305, Japan

and Hyoe Hatakeyama
Industrial Products Research Institute, 1-1-4 Higashi, Tsukuba, Ibaraki 305, Japan
(Received 17 April 1989; revised 7 June 1989; accepted 23 June 1989)

The phase transitions of the water–xanthan system are studied using differential scanning calorimetry (d.s.c.). Upon heating, a glass transition, the cold crystallization of water, melting of water and transition from the mesophase to the isotropic liquid were observed for samples with water content (W_c) ranging from 0.5 to 1.4. These transition temperatures vary depending on the water content. The glass transition was observed for water content ranging from 0.5 to 2.0. Enthalpy relaxation was observed to occur after annealing at a temperature lower than the glass transition temperature. From the heat of fusion of water, the amounts of non-freezing (W_{nf}) and freezing water (W_f) were calculated. There were 50 non-freezing water molecules per repeat unit (four pyranose units). The heat of transition from the mesophase to the isotropic liquid decreased with increasing W_c. The heat capacity difference (ΔC_p) between the glassy and liquid states was measured for the system, and it was found that this showed a good correlation with W_c. The d.s.c. results indicate that both transitions, the liquid crystalline to the isotropic liquid state and the glass.transition, are caused by the molecular motion of xanthan sorbed on non-freezing water.

(Keywords: phase transition; water; xanthan; d.s.c.)

INTRODUCTION

Xanthan is a polysaccharide produced by *Xanthomonas campestris*, which has a rigid cellobiose unit: a trisaccharide side-chain attaches to alternate D-glucosyl residues[1–3] of the main chain. From the X-ray diffraction analysis, it was shown that the crystalline structure of xanthan is a 5_1 helix with 4.7 nm pitch length[4,5]. Recently, the solution properties of xanthan were extensively studied by means of light scattering, sedimentation velocity, optical rotation and viscometry[6–13]. Norisuye *et al.* suggested that xanthan dissolves in 0.1 M aqueous NaCl and takes a rod-like 5_1 double helix[7–9]. A conformational transition of xanthan was thermally induced in dilute solution at around 330 K[10,13,14]. This order–disorder change was thought to be the partial melting of the double helix[14]. It is assumed that the rigid rod of xanthan forms the cholesteric order in aqueous solution[15]; however, the critical condition for the mesophase formation has not been clarified.

It has been reported that high-concentration aqueous solution of polyelectrolytes, such as poly(styrene sulphonate) and cellulose sulphate, show the mesophase at room temperature[16–18]. The phase transition temperature from the mesophase to the isotropic liquid state depends strongly on the water content[18]. The non-freezing water content was calculated from the results of differential scanning calorimetry (d.s.c.) in these polyelectrolyte–water systems. The non-freezing water seems to play an important role in forming the mesophase.

In this study, the phase transition behaviour of the water– xanthan system was investigated as a function of water content. The non-freezing water content was calculated from the heat of fusion of water using d.s.c. In particular, the glass transition behaviour and the transition from the mesophase to the isotropic liquid were analysed as a function of non-freezing water content.

EXPERIMENTAL

Sample

The xanthan used was Kelzan^R, supplied by Kelco Co. Ltd. An aqueous solution of a commercial xanthan (about 1% of polymer) was exposed to 45 kHz ultrasonic irradiation for 0.5 h at 300 K using a Bransonic model B-2200. After the irradiation, the solution was poured into a large quantity of acetone to precipitate the polymer. The polymer obtained was carefully dried at a temperature below 300 K over phosphorus pentoxide (P_2O_5) *in vacuo*.

The purified sample was weighed and dissolved in distilled water in a d.s.c. aluminium sample vessel. After completely dissolving, the water was slowly evaporated in order to fix the water content. Before d.s.c. measurement, all samples were kept at 300 K for a few days in order to homogenize samples.

Measurement of ion content

The content of sodium and potassium in xanthan was measured using a Shimadzu flame emission spectrophotometer model AA-670. The measurement was carried out

0032-3861/90/040693-06

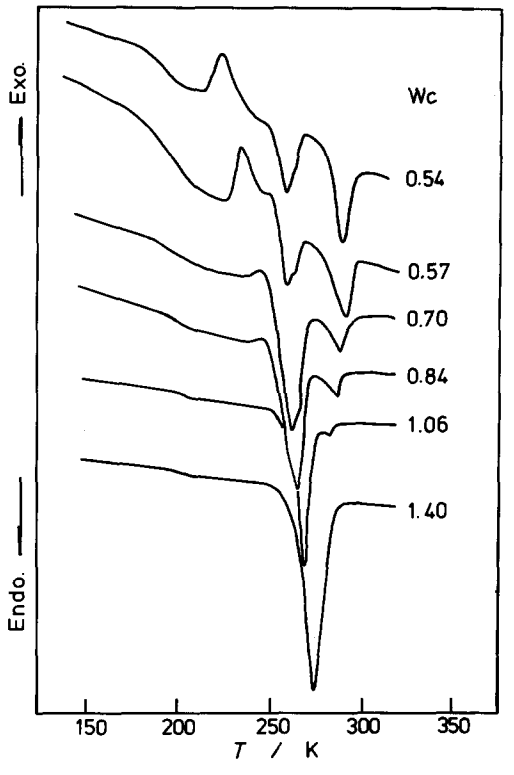

Figure 1 D.s.c. heating curves of the water–xanthan system with various water contents. Water content (W_c) of each sample is shown in the figure

with an air–acetylene flame at 589.0 nm for sodium and at 766.5 nm for potassium.

Differential scanning calorimetry

The d.s.c. used throughout the experiment was a Seiko DSC 200 combined with a Seiko Thermal Analysis System SSC 5000. The measurement was carried out at 10 K min^{-1}. The water content (W_c) was defined as follows:

$$W_c\ (g/g) = w_w/w_s\ (g/g) \quad (1)$$

where w_w is weight of water in the system and w_s is that of the completely dry sample. The dry sample weight was determined from the weight after heating up to 460 K, at which the endothermic peak due to the evaporation of water disappeared completely.

RESULTS AND DISCUSSION

From the flame emission spectrophotometer analysis, the number of sodium ions per repeat unit of xanthan (for four pyranose units) was 2.6 and the number of potassium ions was almost negligible.

The d.s.c. heating curves of samples with various water contents are shown in *Figure 1*. All samples were prepared by cooling from 300 K to 150 K at 10 K min^{-1}. A glass transition also was found in d.s.c. curves of samples having $W_c < 0.5$. This fact suggested that water molecules at concentration $W_c < 0.5$ did not crystallize. As mentioned in our previous papers[16–20], this type of water is categorized as non-freezing water. For the sample with $W_c = 0.54$, the heat capacity jump, the exothermic peak and two endothermic peaks were observed from the low-temperature to the high-temperature side. With increasing W_c, as shown in the sample with $W_c = 1.4$, the exothermic peak disappeared. At the same time, the endothermic peak that appeared at the high-temperature side was difficult to detect. These four transitions were attributed to the glass transition, cold crystallization, melting of water and transition from the mesophase to the isotropic liquid state, respectively, as explained in the following section.

When samples having W_c from 0.5 to 1.4 were cooled at 10 K min^{-1} from room temperature to 180 K, the broad exothermic peak, which corresponded to the crystallization of water, was observed at around 240 K on the d.s.c. cooling curve as shown in *Figure 2*. The T_m of samples having W_c from 0.5 to 1.4 was lower than that of pure water. On the other hand, a sharp exothermic peak was observed at around 250 K, when the sample having $W_c > 1.4$ was cooled at 10 K min^{-1}.

These transition temperatures obtained from the d.s.c. heating curves were plotted against W_c. *Figure 3* shows the results obtained from the heating curves. The glass transition temperature (T_g) was defined as the intersection of extrapolations of the baseline and slope. The other three transition temperatures were defined as the peak temperatures. The melting temperature of water (T_m) depended on W_c in the W_c region below 1.4. As shown in *Figure 3*, the T_m of samples having W_c ranging from 0.5 to 1.4 was lower than that of pure water. In the same W_c range, the cold crystallization temperature (T_{cc}) also showed marked W_c dependence. From these facts, it is suggested that water molecules in the systems with W_c between 0.5 and 1.4 are strongly affected by the existence of xanthan molecules. These kinds of water molecules can also be categorized as bound water. On this account, at least two types of bound water are defined: one is non-freezing water and the other is freezing bound water, the melting and crystallization temperatures of which are lower than those of pure water. The phase diagram shown in *Figure 3* also indicates that the samples with $W_c > 1.4$

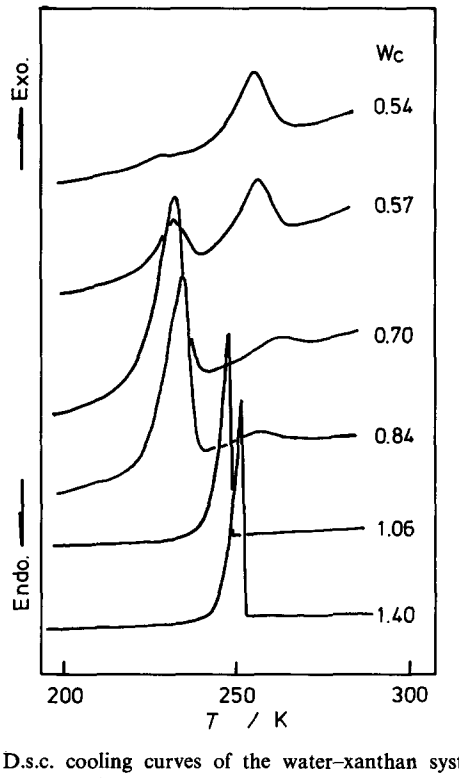

Figure 2 D.s.c. cooling curves of the water–xanthan system with various water contents

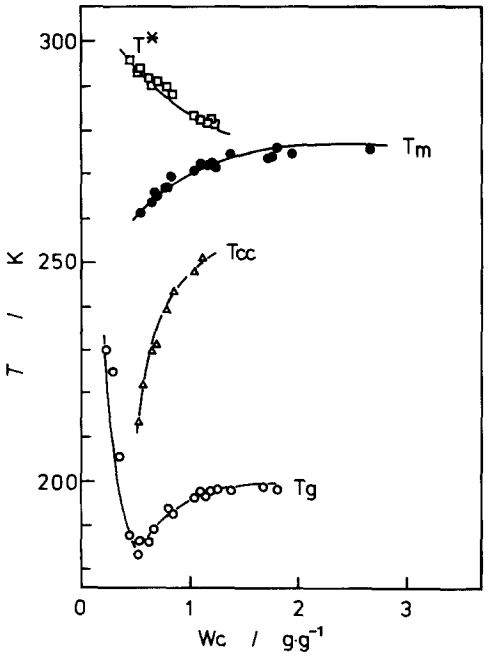

Figure 3 Relationship between phase transition temperatures and water content for the water–xanthan system: T_g, glass transition; T_{cc}, cold crystallization; T_m, melting; T^*, transition from the mesophase to the isotropic liquid state

contain free water in addition to non-freezing and freezing bound water.

From the heat of fusion of water, the total amount of freezing water in the sample was calculated. The freezing water content (W_f) and the non-freezing water content (W_{nf}) were defined as follows:

$$W_{nf} = W_c - W_f \quad (2)$$

W_{nf} and W_f are shown as a function of W_c in *Figure 4*. As shown in the figure, only W_{nf} increases with increasing W_c in the W_c region below 0.5. Above $W_c = 0.5$, W_{nf} increases slightly. When the linear relationship between W_{nf} and W_c in the W_c range above 0.5 was extrapolated to the ordinate, 0.49 (g/g) was obtained. From this value, there were ~50 non-freezing water molecules per repeat unit of xanthan. It is known that, in the case of hydrophilic polymers, one hydroxyl group absorbs one non-freezing water molecule[17,19,20]. As each repeat unit of xanthan (four pyranose units) used in this study contained 2.6 sodium ions, it was estimated that one sodium ion was surrounded by about 10 non-freezing water molecules. The amount of non-freezing water molecules per sodium ion in xanthan depended on the degree of substitution with the pyruvate group and the number of carbonyl and ether groups. Some polyelectrolytes with sodium as the counterion, such as poly(styrene sulphonate) and carboxy methylcellulose, have seven or eight molecules of non-freezing water per sodium ion[21]. The above data also support the idea that the estimated value of number of water molecules around the sodium ion in the water–xanthan system is reasonable.

As shown in d.s.c. curves in *Figure 1*, the water–xanthan systems with W_c ranging from 0.45 to 1.2 showed an endothermic peak at a temperature higher than T_m. When the sample having $W_c = 1.0$ was observed with a polarizing light microscope at 293 K, the liquid-crystalline texture was observed. *Figure 5* shows polarizing light micrographs taken under crossed Nicols. From these micrographs, it is reasonable to consider that the phase which appeared in W_c ranging from 0.45 to 1.0, and in the temperature range from 300 to 260 K shown in *Figure 3*, is attributable to the liquid-crystalline phase. As shown in *Figure 3*, the transition temperature from the mesophase to the isotropic liquid state (T^*) decreased with increasing W_c. Similar phase diagrams were also found for the other water–polyelectrolyte systems, such as water–sodium cellulose sulphate, water–sodium carboxymethylcellulose, water–poly(styrene sulphonate) systems, etc.[16–18].

The heat of transition (ΔH^*) from the mesophase to the isotropic liquid state was calculated from the peak area of the d.s.c. curves. When ΔH^* (J g^{-1}) is calculated, the heat obtained is normalized using the total weight of the system. However, the data obtained showed no relationship with W_c, when the total weight of the system was used in this study. In contrast, when the weight summation of dry xanthan and non-freezing water was used, the calculated values showed a good accordance with W_c. *Figure 6* shows the normalized heat of transition (ΔH^*) as a function of W_c. As shown in *Figure 6*, the value of ΔH^* decreased with increasing W_c. The results of *Figure 6* indicate a W_c dependence of T^*, suggesting that liquid-crystal formation depended strongly on W_c. Therefore, the liquid-crystalline phase observed in this study is thought to be the lyotropic nematic structure formed by xanthan molecules absorbing non-freezing water. A texture similar to the pattern shown in *Figure 5* was found not only in the water–xanthan system but also in other water–polyelectrolyte systems, such as water–sodium poly(styrene sulphonate), water–sodium carboxymethylcellulose[22,23]. Judging from our experimental results, characteristic features indicating the cholesteric phase were not observed, even when the samples ($W_c = 0.6$–1.2) were maintained at 296 K for three weeks. Therefore, it is assumed that the texture observed by the polarizing microscope suggests the existence of the nematic liquid crystal, the type of mesophase of the water–polyelectrolyte systems.

The d.s.c. curves of samples having various thermal histories are shown in *Figure 7*. The W_c of the sample shown in this figure was 0.7. When the sample was cooled at 10 K min^{-1} from the isotropic liquid state, two exothermic peaks were observed on the d.s.c. cooling curve. The small exothermic peak at 270 K is due to the

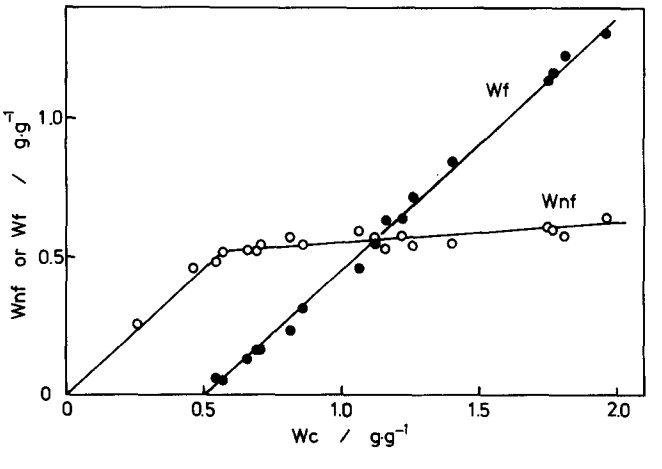

Figure 4 Relationship between non-freezing (W_{nf}) and freezing (W_f) water contents and water content (W_c) of water–xanthan system

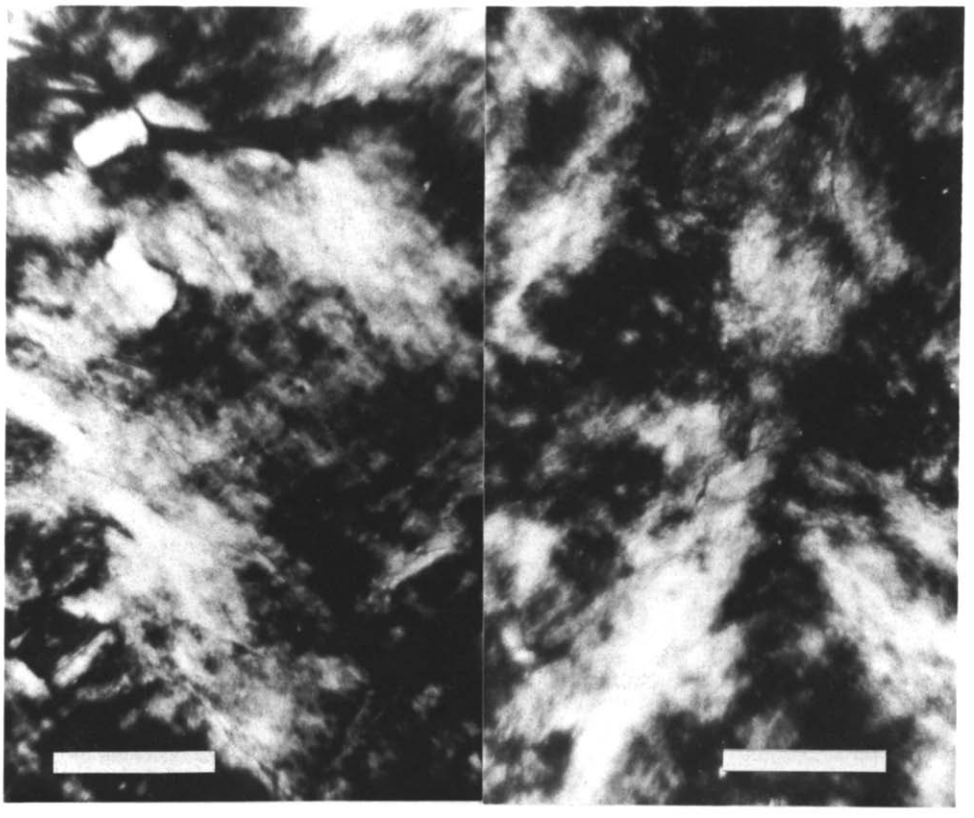

Figure 5 Polarizing light micrographs of the water–xanthan system: $W_c \simeq 1.0$, $T = 293$ K, scale = 100 μm

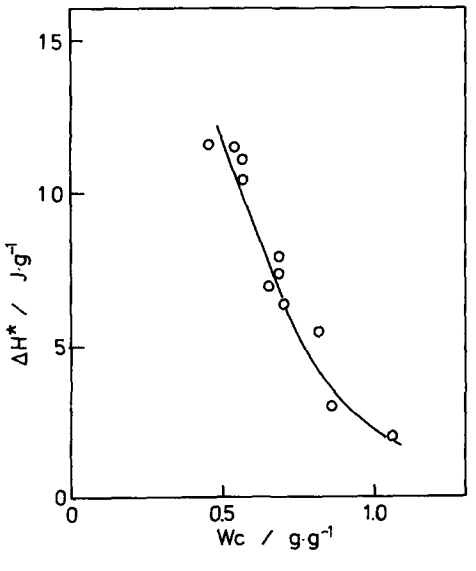

Figure 6 Relationship between heat of transition from mesophase to isotropic liquid state (ΔH^*) and water content (W_c)

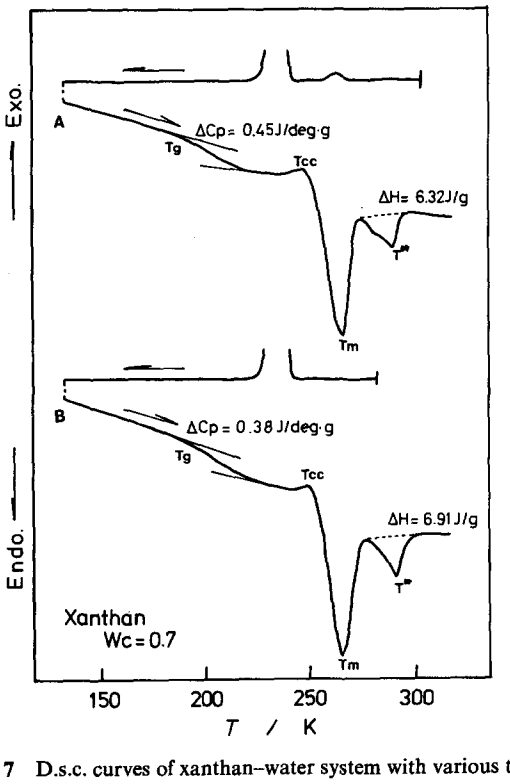

Figure 7 D.s.c. curves of xanthan–water system with various thermal histories

transition from the isotropic liquid state to the liquid-crystalline phase, and the other peak at around 240 K is due to the crystallization of water. When the sample was heated at 10 K min^{-1} from 140 K, d.s.c. curve A was obtained. In the case of curve B, the sample was cooled from the liquid-crystalline phase instead of from the isotropic liquid phase. The transition from isotropic state to liquid-crystalline phase was not observed on the d.s.c. cooling curve. Both T_{cc} and T_m were not affected by thermal history. However, T^* of the sample cooled from the isotropic state (A) shifted to lower temperature to a greater degree than that of the sample cooled from the liquid-crystalline phase (B). The endothermic peak from the liquid-crystalline to the isotropic liquid phase of curve A was broader than that of curve B. The heat of transition of curve A, which was normalized by the total weight of dry xanthan and non-freezing water, was smaller than that of curve B. These facts suggested that the liquid-

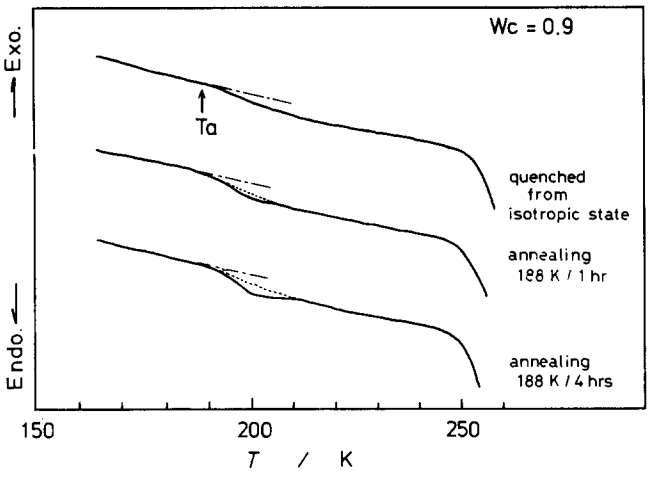

Figure 8 D.s.c. curves of xanthan–water system with various degrees of enthalpy relaxation

crystalline state of the sample cooled from the isotropic liquid state is more random than that of the sample cooled from the liquid-crystalline phase.

The structural change of the liquid-crystalline phase reflecting thermal history seems to affect the structure of the glassy state. The glass transition temperature (T_g) of curve A was almost the same as that of curve B. However, the heat capacity difference (ΔC_p) between the glassy and the liquid state at T_g was influenced by thermal history. The value of ΔC_p of curve A was larger than that of curve B. In the case of A, it was considered that large numbers of molecular chains were frozen in a random arrangement, as they could not form the liquid-crystalline phase during rapid cooling. The glass transition was observed in the water–xanthan system at a temperature below 200 K in the W_c range from 0.4 to 2.0. It is known that the glassy state is the non-equilibrium state, having excess thermodynamic quantities such as enthalpy and volume. When the glassy molecular chain was annealed at a temperature lower than T_g, the excess thermodynamic quantities decreased. This phenomenon is known as enthalpy relaxation[24] and volume relaxation[25]. In order to confirm enthalpy relaxation of the water–xanthan system, the sample was annealed under the following conditions. The sample with $W_c = 0.9$, which was quenched from the isotropic liquid state (T_g was 192 K), was annealed at 188 K for different periods. After annealing, the sample was cooled to 160 K and then the d.s.c. curve was obtained by heating. As shown in *Figure 8*, the d.s.c. curves of both annealed samples show a small endothermic peak just above T_g. The broken curves show d.s.c. curves of the quenched sample. This endothermic peak was attributable to enthalpy relaxation of the system. Besides enthalpy relaxation, T_g of the water–xanthan system shifted to the high-temperature side as heating rate increased. These facts show that the water–xanthan system forms the glassy state by quenching and the step-like change of heat capacity is due to glass transition.

As shown in *Figure 1*, the exothermic peak due to the cold crystallization of water was observed for samples having W_c between 0.4 and 1.0. It is also known that the cold crystallization peak was easily influenced by annealing in many glassy organic materials. In order to estimate the effect of annealing on the structural change of the water–xanthan system, the system was annealed and the effect of annealing on the glass transition behaviour was examined. Quenched samples having various W_c values were heated from 150 K to the predetermined annealing temperature, at which the cold crystallization was completely finished, and then quenched to 150 K. The cold crystallization was no longer observed in the annealed samples during heating d.s.c. runs. Both the original and annealed samples showed a glass transition. However, the T_g of the annealed sample shifted to the higher-temperature side and the heat capacity difference (ΔC_p) between the glassy and liquid states at T_g decreased after annealing.

The change of T_g with W_c is shown in *Figure 9*. The samples having W_c from 0.4 to 1.0 showed cold crystallization. The full and open circles show the T_g of the original (with T_{cc}) and annealed samples (without T_{cc}), respectively. The samples having W_c either less than 0.4 or W_c more than 1.0 did not show cold crystallization, as shown in *Figure 1*. The open circle with the vertical line through it (*Figure 9*) indicates the T_g of the samples that did not show the T_{cc}. The original sample was cooled at 10 K min^{-1} from the isotropic liquid state. In the W_c range below 0.4, the T_g of the sample decreased remarkably with increasing W_c. After reaching a minimum value, T_g approached a constant value. The minimum value of T_g corresponded to the temperature where freezing water was formed during cooling. The original samples were prepared by cooling at 10 K min^{-1} from 300 K to 150 K. The exothermic peak due to the crystallization of water was observed on the d.s.c. cooling curve for samples having $W_c > 0.6$. The presence of ice will probably restrict the molecular motion of polysaccharide. Therefore, the T_g of samples having $W_c > 0.6$ increased and approached a constant value. The T_g of the annealed sample was higher than that of the original sample. After reaching the minimum value, T_g approached a constant value, which was the same value as observed for the original sample.

The heat capacity difference (ΔC_p) between the glassy and the liquid states at T_g was calculated. Similar to the ΔH^* normalizing calculation, the ΔC_p was also calculated using the total weight of dry xanthan and non-freezing water. These calculated values are plotted against W_c in *Figure 10*. In this figure, the full circles show ΔC_p of the original samples and the open circles show that of the annealed samples having W_c from 0.4 to 1.0, respectively. The open circle with the vertical line through it (*Figure 10*) indicates the ΔC_p of the samples that showed no T_{cc}. The value of ΔC_p of the original sample decreased

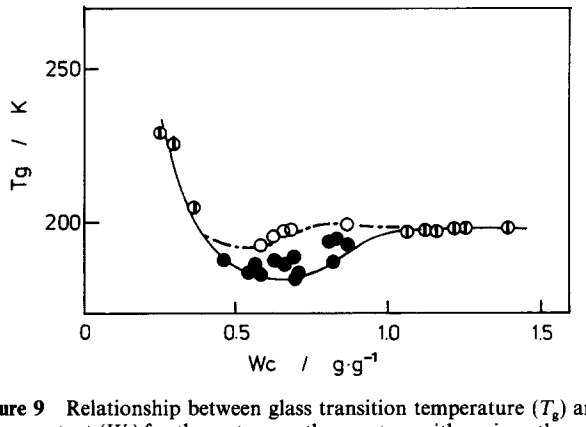

Figure 9 Relationship between glass transition temperature (T_g) and water content (W_c) for the water–xanthan system with various thermal histories: (●) quenched and (○) annealed with cold crystallization; (Φ) without cold crystallization

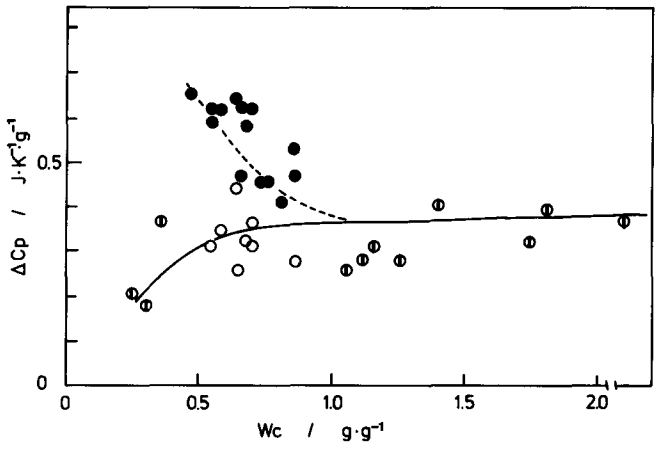

Figure 10 Relationship between heat capacity difference (ΔC_p) at T_g and water content (W_c) of water–xanthan system: (●) quenched and (○) annealed with cold crystallization; (Φ) without cold crystallization

gradually with increasing W_c from 0.5 to 1.2, and then saturated to 0.35 $J K^{-1} g^{-1}$ at a W_c higher than 1.2. This tendency agreed well with the W_c dependence of T_g as shown in *Figure 9*. The results observed in *Figures 9* and *10* suggest that the glass transition of the water–xanthan system reflected the molecular motion of xanthan-sorbed non-freezing water, as well as the transition from the liquid-crystalline state to the isotropic liquid state.

The ΔC_p values of common polymers such as polystyrene[26], poly(alkyl methacrylates)[27] and their oligomers[28] are known to range from 0.18 to 0.36 $J K^{-1} g^{-1}$. The ΔC_p values of the quenched water–xanthan systems ranging from 0.4 to 1.0, as shown in *Figure 10*, seem to be too large compared with the ΔC_p values of common polymers. It is also known that samples having low T_g show large ΔC_p values. Ichihara[29] and the present authors[30] reported a good relationship between $\ln(\Delta C_p)$ and T_g for various samples including polymers and low-molecular-weight materials. Even if the low T_g values of the water–xanthan system are taken into consideration, the ΔC_p values of the original sample seem to be rather high. When the original samples were annealed, the ΔC_p values decreased and reached an almost similar value to that in other glassy materials. In order to explain this phenomenon, we considered cold crystallization of the system. Part of the non-freezing water rearranged into the crystalline state at cold crystallization. As mentioned above, cold crystallization could be observed only for the quenched samples (original samples) with W_c from 0.4 to 1.0. Assuming that the amount of water reflecting cold crystallization is frozen in the glassy state at a temperature below T_{cc}, this amount is concerned in the glass transition.

The amount of glassy water was estimated from the heat of cold crystallization of the original sample. The estimated value of ΔC_p due to the glassy water varied from 3.0 $J K^{-1} g^{-1}$ to 2.1 $J K^{-1} g^{-1}$ as a function of W_c. With increasing W_c, the calculated value of ΔC_p of glassy water approached 2.1 $J K^{-1} g^{-1}$. This value is the same as the ΔC_p value of amorphous ice, which was obtained by sublimation[31]. This fact indicated that a part of the non-freezing water rearranged into the crystalline state during heating. The part of the non-freezing water capable of rearrangement contributed to the increase in ΔC_p at T_g. The glass transition of the original sample was the result of the molecular motion of xanthan, non-freezing water and glassy water.

The results obtained above indicated that the xanthan–water system showed unique phase transition behaviour depending on W_c and thermal history. The structural change of water in the system is a major factor in the formation of glassy and liquid-crystalline phases.

ACKNOWLEDGEMENTS

The authors are grateful to Professor J. Nakamura (Ohtsuma Women's University) for his helpful discussions.

REFERENCES

1 Jeanes, A., Pittsley, J. E. and Senti, F. R. *J. Appl. Polym. Sci.* 1961, **5**, 519
2 Sloneker, J. H. and Jeanes, J. *Can. J. Chem.* 1962, **40**, 2066
3 Jansson, P. E., Goodall, D. M., Morris, E. M. and Rees, D. A. *J. Chem. Soc. Chem. Commun.* 1980, 545
4 Moorhouse, R., Walkinshaw, M. D. and Arnott, S. *ACS Symp. Ser.* 1977, **45**, 90
5 Okuyama, K., Arnott, S., Moorhouse, R., Walkinshaw, M. D., Atkins, E. D. T. and Wolf-Ullish, C. *ACS Symp. Ser.* 1980, **141**, 411
6 Sato, T., Norisuye, T. and Fujita, H. *Polym. J.* 1984, **16**, 341
7 Sato, T., Kojima, S., Norisuye, T. and Fujita, H. *Polym. J.* 1984, **16**, 423
8 Sato, T., Norisuye, T. and Fujita, H. *Macromolecules* 1984, **17**, 2629
9 Sato, T., Norisuye, T. and Fujita, H. *Polym. J.* 1985, **17**, 729
10 Kitagawa, H., Sato, T., Norisuye, T. and Fujita, H. *Carbohydr. Polym.* 1985, **5**, 407
11 Sho, T., Sato, T. and Norisuye, T. *Biophys. Chem.* 1986, **25**, 307
12 Zhang, L., Liu, W., Norisuye, T. and Fujita, H. *Biopolymers* 1987, **26**, 333
13 Liu, W., Sato, T., Norisuye, T. and Fujita, H. *Carbohydr. Res.* 1987, **160**, 267
14 Paoletti, S., Cesaro, A. and Dellen, F. *Carbohydr. Res.* 1983, **123**, 173
15 Maret, G., Milas, M. and Rinaudo, M. *Polym. Bull.* 1981, **4**, 291
16 Hatakeyama, T., Nakamura, K., Yoshida, H. and Hatakeyama, H. *Thermochim. Acta* 1985, **88**, 223
17 Hatakeyama, H., Yoshida, H. and Hatakeyama, T. 'Cellulose and its Derivatives' (Ed. J. F. Kennedy), Wiley, Chichester, 1985, p. 255
18 Hatakeyama, T., Yoshida, H. and Hatakeyama, H. *Polymer* 1987, **28**, 1282
19 Nakamura, K., Hatakeyama, T. and Hatakeyama, H. *Polymer* 1983, **24**, 871
20 Nakamura, K., Hatakeyama, T. and Hatakeyama, H. *Polym. J.* 1983, **15**, 361
21 Nakamura, K., Hatakeyama, T. and Hatakeyama, H. 'Wood and Cellulosics' (Ed. J. F. Kennedy), Ellis Horwood, Chichester, 1987, p. 97
22 Hatakeyama, H. *Kagaku to kogyo* 1989, **42**, 878
23 Hatakeyama, T., Yoshida, H. and Hatakeyama, H. *Food Hydrocolloids*, 1989, **3**, 301
24 Suga, H. and Seki, S. *J. Non-Cryst. Solids* 1974, **16**, 171
25 Kovacs, A. J. *J. Polym. Sci.* 1958, **30**, 131
26 Yoshida, H. *Netsu Sokutei* 1986, **13**, 191
27 Yoshida, H. and Kobayashi, Y. *J. Macromol. Sci.—Phys. (B)* 1982, **21**, 565
28 Yoshida, H. and Kobayashi, Y. *Polym. Eng. Sci.* 1983, **23**, 907
29 Ichihara, S. *Netsu Sokutei no Shipo* 1986, **4**, 1
30 Hatakeyama, T., Nakamura, K., Yoshida, H., Hirose, S. and Hatakeyama, H. 'Proc. Soc. Thermal Analysis and Calorimetry, Japan', Tokyo, 1988, p. 124
31 Sugisaki, M., Suga, H. and Seki, S. *Bull. Chem. Soc. Japan* 1968, **41**, 2591